The DC-Link Capacitor Current in Pulsed Single-Phase H-Bridge Inverters

Folker Renken
Siemens VDO Automotive AG
Automotive Systems Powertrain
Siemensstraße 12
93055 Regensburg, Germany
Phone: ++49 941 790 5385
E-mail: folker.renken@siemens.com

Acknowledgments

I thank Mr. Werner Mißfeldt from the Helmut-Schmidt-University Hamburg for the practical measurements. The analytical calculations are compared with these measurements in the paper.

Keywords

«Uninterruptible power supplies (UPS)», «Converter circuits», «High frequency power converter», «Power transmission», «Harmonics», «Measurements»

Abstract

In case of controlling a pulsed single-phase H-bridge inverter with two and three voltage levels the capacitor currents in the dc-link circuit are calculated analytically. For these calculations first a sinusoidal modulated voltage and sinusoidal current at the output of the inverter are presupposed. Afterwards the additional load of the dc-link capacitors caused by harmonic currents of the output filter circuit is examined. For this reason the individual harmonics of the dc-link current with sinusoidal and with overlaid harmonic output currents are calculated with help of spectral analysis. At last the influence of the switching processes to the dc-link circuit load is discussed. The theoretically determined currents in the dc-link capacitors are compared with several practical measurements.

Introduction

In pulsed voltage source inverters the dc-link capacitors contributes substantially to the volume, the weight and the costs. For this reason the necessary amount of capacitors has to be determined exactly to prohibit over design if possible [1]. In most applications the capacitor design is crucially determined by the load current. For this reason the capacitor current in pulsed single-phase H-bridge inverters for different control strategies is analytical calculated in this paper. The power stage of the pulse inverter is presented in the following figure. It consists of an inverter bridge, an input circuit with dc-link capacitors and a filter circuit on the output side.

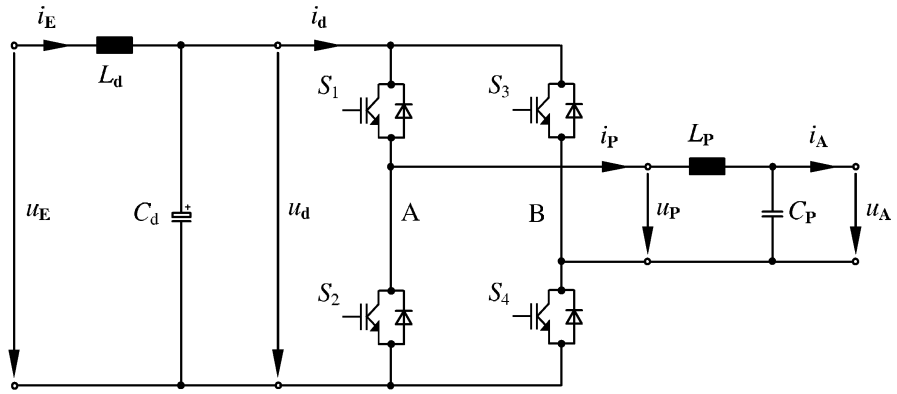

Fig. 1: Power stage of a pulsed H-bridge inverter with input and output filter circuit

First for the calculation an ideal sinusoidal modulated voltage u_P and a sinusoidal current i_P with any phase angle at the inverter output is supposed. Afterwards the influence of the harmonic current by the output filter circuit of the inverter is calculated. Also the load of the dc-link capacitors by switching transitions in the H-bridge is examined. All the calculation results are verified by several practical measurements. The valid inverter control schemes for the calculations are introduced in the next chapter.

Control Schemes for a Single Phase H-Bridge Inverter

The following figure shows two pulse control schemes of a single phase H-bridge inverter. On the left the output voltage of the inverter bridge is controlled by two voltage levels; on the right by three voltage levels. With the control scheme for two voltage levels both inverter-legs are switched at the same time with the output pulse frequency of the inverter. Thereby the two half-bridges are switched inverted to each other. That means if the voltage on one bridge-leg is high the voltage at the other bridge-leg is zero and reversed. The difference of the voltage from both bridge-legs results in the output voltage of the inverter bridge u_P with the two voltage levels $+u_{d-}$ und $-u_{d-}$. With that control scheme with three voltage levels in the figure right both inverter-legs are only pulsed with the half output frequency of the inverter. While one inverter-leg is pulsed with a long pulse, the other bridge-leg is pulsed with a short pulse. The difference of the two pulses results in two new pulses at the bridge output. After each half fundamental period the pulse lengths of the two bridge-legs are exchanged, so that the resulting voltage gets another polarity. In this way the output voltage u_P is produced with three voltage levels $+u_{d-}$, 0 und $-u_{d-}$.

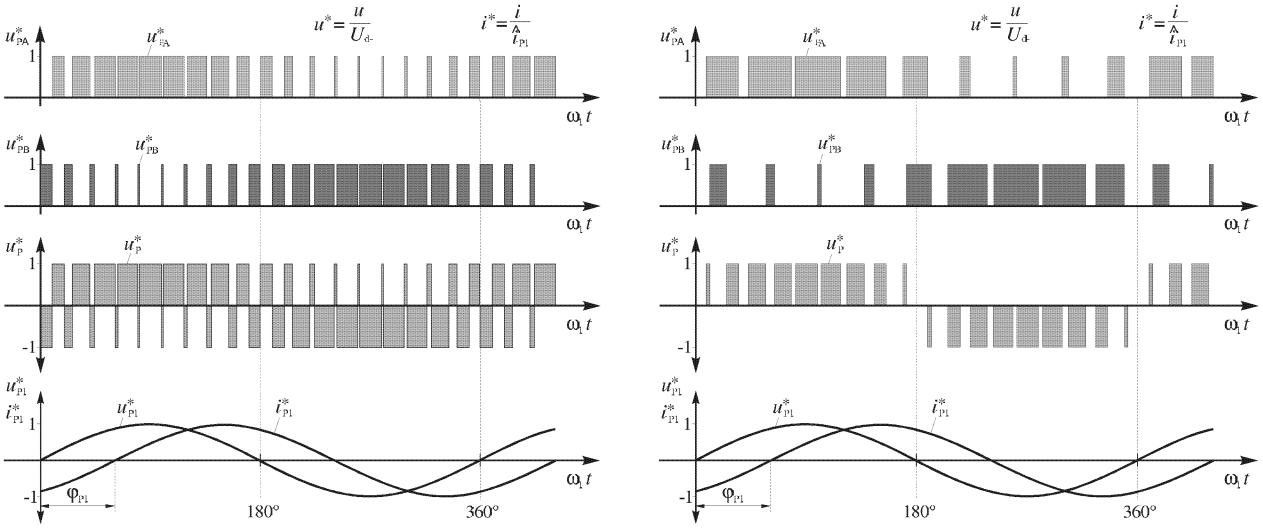

Fig. 2: Voltage- and current waveforms of a single phase H-bridge inverter for sine-modulated pulse control schemes with two (left) and three voltage levels (right)

Below in the figure for both control schemes the sinusoidal fundamental portion of the output voltage u_{P1} is presented. Besides the voltage a sinusoidal output current i_{P1} with a phase shift angle is shown. For this output current waveform of the inverter first the dc-link current load will be determined.

DC-Link Current of the Inverter with Sine Wave Output Current

Now for control with two and three voltage levels the current in the dc-link circuit for a single phase H-bridge inverter will be calculated. Beside a sinusoidal duty cycle shape that means a sinusoidal modulated voltage u_P, a sinusoidal current i_P at the output of the inverter bridge is assumed. Moreover, the dc-link voltage u_d is presumed as constant. With these conditions the input current of the inverter can be split in a dc-component, in an ac-component with double fundamental frequency and in a higher-frequent component [2, 3, 4, 5]. For control with two voltage levels the input current of the single phase inverter is split into individual components for ohmic - and inductive load in figure 3.

 ISBN : 90-75815-08-5

The middle part of the figure shows the current pulses at the input of the inverter. The positive and negative sinusoidal current at the output build here the envelope curve for the inverter input pulses. The instantaneous value of the current in the pulse periods is dependent on the amplitude $\hat{\imath}_{P1}$, the phase shift angle φ_{P1} and the actual duty cycle of the modulation factor m.

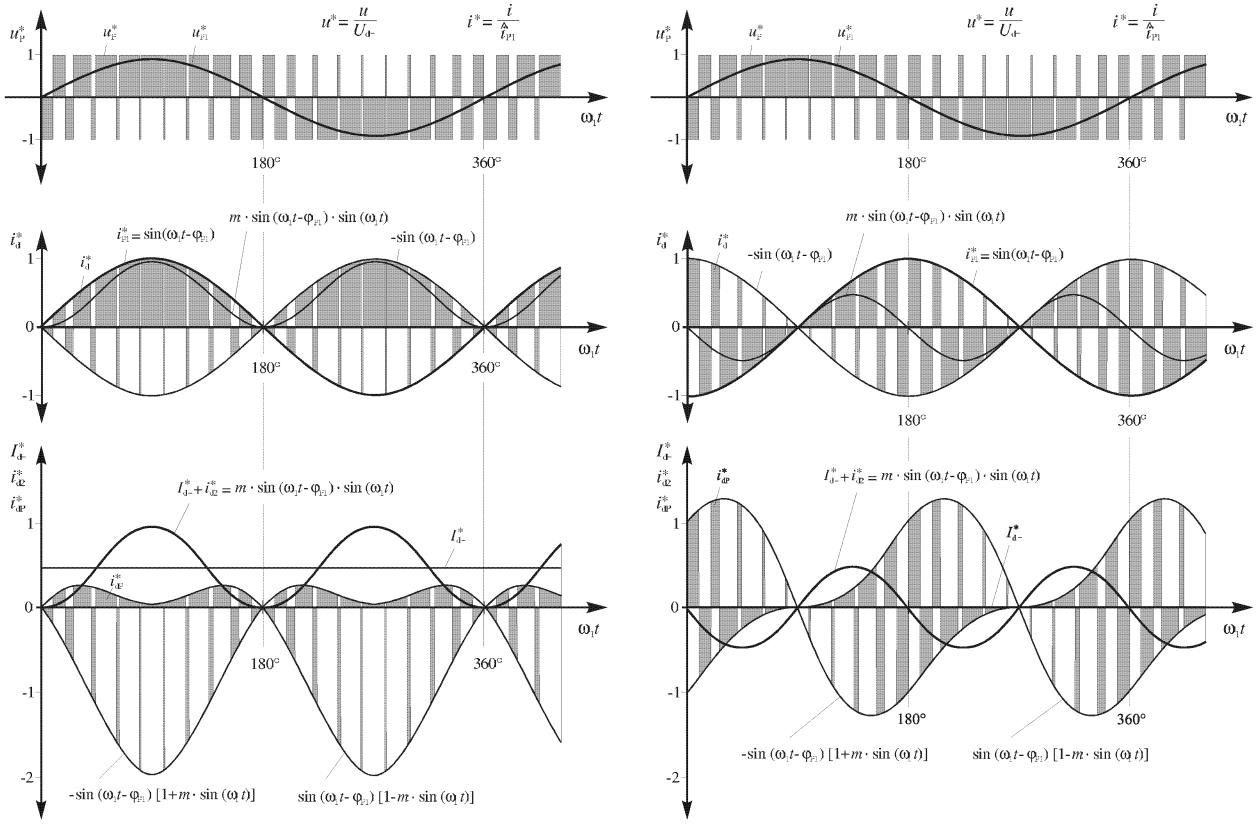

Fig. 3: Input current i_d and its split into the individual components of a two voltage level controlled inverter with a phase shift angle of $\varphi_{P1} = 0°$ (left) and $\varphi_{P1} = 90°$ (right) [2]

In the following formulas the waveform of the current and the related duty cycles in the switch-on state - that means connection to positive - and switch-off state - the connection to negative terminal of dc-link capacitors - are shown.

Current - and duty cycle waveforms in the switch-on state:

$$i_{de}(t) = \hat{i}_{P1} \cdot \sin(\omega_1 t - \varphi_{P1}) \tag{1}$$

$$\frac{t_e(t)}{T_P(t)} = \frac{1}{2} \cdot \left[1 + m \cdot \sin(\omega_1 t)\right] \tag{2}$$

Current - and duty cycle waveforms in the switch-off state:

$$i_{da}(t) = -\hat{i}_{P1} \cdot \sin(\omega_1 t - \varphi_{P1}) \tag{3}$$

$$\frac{t_a(t)}{T_P(t)} = \frac{1}{2} \cdot \left[1 - m \cdot \sin(\omega_1 t)\right] \tag{4}$$

$$\text{for} \quad 0 \le m \le 1 \quad \text{and} \quad -180° \le \varphi_{P1} \le 180°$$

The average-value of the current pulse in each individual period results in a waveform it consists of a dc-current which is superimposed by an alternating current with double fundamental frequency $[I_{d-} + i_{d2}(t)]$. This current is determined by multiplication of current - and duty cycle waveforms.

$$I_{d-} + i_{d2}(t) = i_{de}(t) \cdot \frac{t_e(t)}{T_P(t)} + i_{da}(t) \cdot \frac{t_a(t)}{T_P(t)} \tag{5}$$

$$I_{d-} + i_{d2}(t) = m \cdot \hat{i}_{P1} \cdot \sin(\omega_1 t - \varphi_{P1}) \cdot \sin(\omega_1 t) \tag{6}$$

The split of this current shows: The dc-component is depended on the phase shift angle φ_{P1} and the modulation factor m. The rms-current of the double fundamental frequency portion however has the

 ISBN : 90-75815-08-5

same value at all phase shift angles φ_{P1} and changes only with the modulation factor m. For control of the inverter with three voltage levels these components has the same results [2, 6, 7].

The dc-current I_{d-} and the double fundamental frequency current $I_{d2}(t)$:

$$I_{d-} = \frac{m \cdot \hat{i}_{P1}}{2} \cdot \cos(\varphi_{P1}) \tag{7}$$

$$I_{d2} = \frac{m \cdot \hat{i}_{P1}}{2 \cdot \sqrt{2}} \tag{8}$$

Now with the low-frequency current waveform of equation 6 the envelopes of the higher-frequency current portion are determined. This can be done by subtraction of the low-frequency current portion from the output current and the inverting output current.

Higher frequency current waveform in the switch-on and switch-off state:

$$i_{dOe}(t) = \hat{i}_{P1} \cdot \sin(\omega_1 t - \varphi_{P1}) \cdot [1 - m \cdot \sin(\omega_1 t)] \tag{9}$$

$$i_{dOa}(t) = -\hat{i}_{P1} \cdot \sin(\omega_1 t - \varphi_{P1}) \cdot [1 + m \cdot \sin(\omega_1 t)] \tag{10}$$

The rms-value of the higher-frequency current can be determined by the current waveforms and the appropriate duty cycles in the switch-on and -off condition within a half fundamental period. For this the integral for the pulses in switch-on - and switch-off state is made and then the arithmetic sum of the two partial values is calculated.

$$I_{dO}^2 = \frac{1}{\pi} \cdot \int_0^{180°} \left[i_{dOe}^2(t) \cdot \frac{t_e(t)}{T_P(t)} + i_{dOa}^2(t) \cdot \frac{t_a(t)}{T_P(t)} \right] d\omega_1 t \tag{11}$$

$$I_{dO} = \hat{i}_{P1} \cdot \sqrt{\frac{1}{8} \cdot [4 - m^2 \cdot (1 + 2 \cdot \cos(\varphi_{P1})^2)]} \tag{12}$$

The higher frequency current in the dc-link circuit is dependent on the fundamental phase angle φ_{P1} and the modulation factor m. The maximum value of this current is $I_{do\,max} \approx 0.71\ \hat{i}_{P1}$. The calculation of the higher frequent current for control of the inverter with three voltage levels results to [2, 6, 7]:

$$I_{dO} = \hat{i}_{P1} \cdot \sqrt{\frac{m}{24 \cdot \pi} \cdot [24 - 6 \cdot \pi \cdot m + (8 - 3 \cdot \pi \cdot m) \cdot \cos(2\varphi_{P1})]} \tag{13}$$

For this control scheme the higher frequency current in the dc-link circuit is also dependent on the phase angle φ_{P1} and the modulation factor m. But the maximum value is much lower $I_{do\,max} \approx 0.35\ \hat{i}_{P1}$. In figure 4 the rms-component of the higher frequency current in the dc-link circuit for control of the inverter with two (left) and three voltage levels (right) are compared to each other. Over wide ranges the current value in the dc-link circuit for three voltage levels compared to that with two voltage levels is clearly smaller.

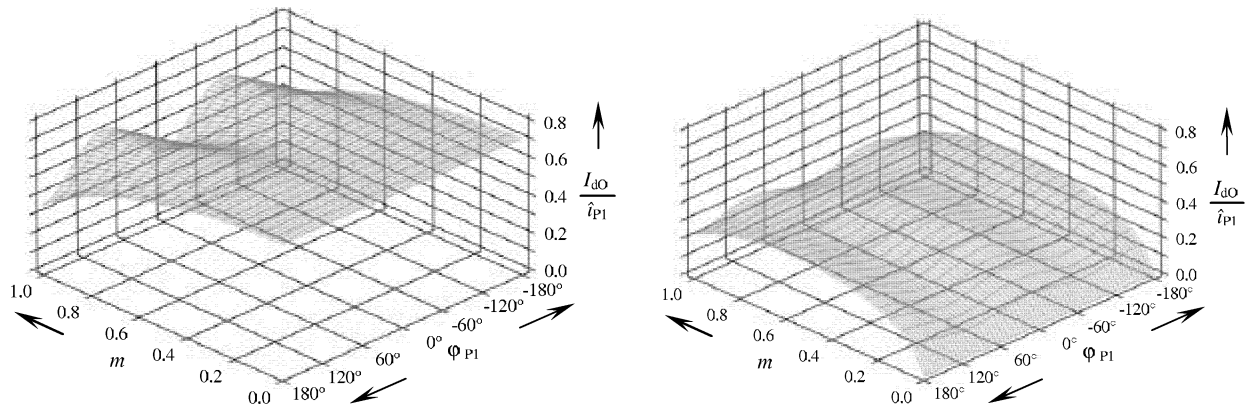

Fig. 4: Higher-frequency rms-current in the dc-link circuit for control with two (left) and three voltage levels (right)

As the parasite inductance from the half-bridge to the dc-link circuit usually is very much lower than to the dc-voltage supply (factor > 100) approximately the entire higher-frequency current - presented in the figure - flows though the dc-link capacitor. Beside this current, still another portion of the current with double frequency flows in the dc-link capacitors. This portion depends considerably on inductance L_d in the dc-input of the inverter and can easily be determined from the parallel connection of L_d and C_d. By arithmetic addition of the higher-frequency current portion and the current with double frequency the total value of current in the dc-link circuit capacitors can be determined [2, 8].

DC-Link Current of the Inverter with Output Current Harmonics

The calculation of the dc-link capacitor current is made for a sinusoidal current i_P at the output of the inverter bridge. But also harmonic current in the filter circuit occurs by pulse width modulated voltage. This current and the fundamental current together forms the current output of the H-bridge inverter. The additional load in the dc-link capacitors of these higher-frequency currents will be determined with the help of Fourier analyses.

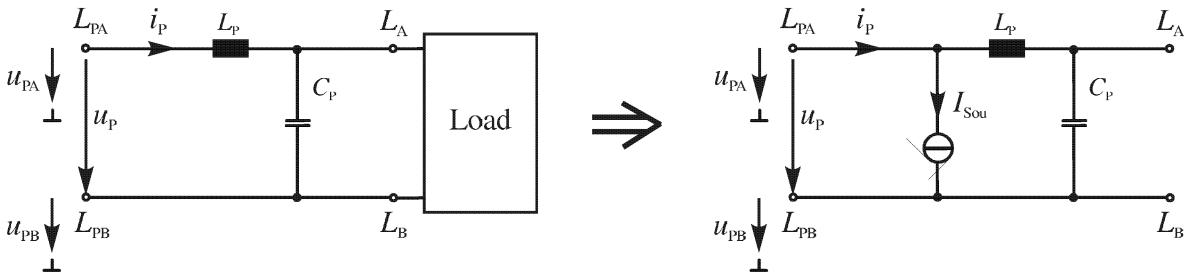

Fig. 5: Inverter filter with load (left) and without load and current source at filter input (right)

In figure 7 (left) the filter circuit of an H-bridge inverter is presented. At the output of these filter circuits the voltage ripple normally is lower than 1% of the nominal sinus output voltage peek value. For this small ripple during the pulse periods a sinusoidal voltage and current waveform at the filter output can be accepted in good approximation. The sinusoidal output current and the harmonic currents in the filter together build the output current of the inverter bridge. So, for calculation an alternative filter circuit can used (figure right). In this mathematical model the filter circuit of the inverter is completely without load at the output. Instead the load a current source $i_{Sou}(t)$ with a fundamental waveform parallel to the filter circuit is used.

$$i_{Sou}(t) = \hat{i}_{Sou} \cdot \cos\left(\omega_1 t - \varphi_{Sou}\right) \tag{14}$$

For the calculation of the dc-link circuit current first the output current of the inverter bridge must be determined. This consists of the sinusoidal load current $i_{Sou}(t)$ and the idle current of the output filter. The sinusoidal current is defined in equation 14. For the calculation of the filter current first the pulsed voltage at the output of the H-bridge must be defined. In case of the control with two voltage levels the Fourier analysis of the voltage at the bridge legs A and B results in the following formulas:

$$u_{PA}(\omega_1 t) = \frac{U_d}{2} \cdot \left[1 + m \cdot \cos(\omega_1 t)\right] + \sum_{\mu=1}^{\infty} \frac{2 \cdot U_d}{\mu \cdot \pi} \cdot \sin\left[\frac{\mu \cdot \pi}{2} \cdot \left[1 + m \cdot \cos(\omega_1 t)\right]\right] \cdot \cos\left[\mu \cdot \left(p \cdot \omega_1 t + \pi\right)\right] \tag{15}$$

$$u_{PB}(\omega_1 t) = \frac{U_d}{2} \cdot \left[1 - m \cdot \cos(\omega_1 t)\right] + \sum_{\mu=1}^{\infty} \frac{2 \cdot U_d}{\mu \cdot \pi} \cdot \sin\left[\frac{\mu \cdot \pi}{2} \cdot \left[1 - m \cdot \cos(\omega_1 t)\right]\right] \cdot \cos\left[\mu \cdot \left(p \cdot \omega_1 t\right)\right] \tag{16}$$

The difference of these two voltages results in the output voltage of the inverter. This is also the input voltage at the output filter. For calculation of the current in the filter circuit the individual oscillations of the voltage must be determined with the help of Bessel functions.

$$u_P(\omega_1 t) = U_d \cdot m \cdot \cos(\omega_1 t) + \sum_{\mu=1}^{\infty} \sum_{\nu=1}^{\infty} \frac{2 \cdot U_d}{\mu \cdot \pi} \cdot \sin\left[\frac{\pi \cdot (\nu - \mu)}{2}\right] \cdot k_\nu \cdot J_\nu\left(\frac{\pi \cdot \nu \cdot m}{2}\right) \cdot \left\{\cos\left[(\mu \cdot \rho - \nu)\omega_1\right] + \cos\left[(\mu \cdot \rho + \nu)\omega_1\right]\right\} \tag{17}$$

 ISBN : 90-75815-08-5

To reach the filter current the individual components of the voltage must be divided by the absolute value of the resistance and supplemented by the appropriate phase shift angle. The fundamental current in the filter is relatively small. For representing the load a fundamental current $i_{Sou}(t)$ is added to the filter current. The sum of these currents results in the output current of the inverter.

$$i_P(\omega_1 t) = \hat{i}_{Sou} \cdot \cos(\omega_1 t - \varphi_{Sou}) + \frac{U_d \cdot m}{|Z_{PF}|} \cdot \cos(\omega_1 t - \varphi_{PF}) + \sum_{\mu=1}^{\infty} \sum_{\nu=1}^{\infty} \frac{2 \cdot U_d}{\mu \cdot \pi} \cdot \sin\left[\frac{\pi \cdot (\nu - \mu)}{2}\right] \cdot k_\nu \cdot J_\nu\left(\frac{\pi \cdot \nu \cdot m}{2}\right) \cdot \left\{\frac{1}{|Z_{PO-}(\mu,\nu)|} \cdot \cos\left[(\mu \cdot \rho - \nu)\omega_1 - \varphi_{PO-}(\mu,\nu)\right] + \frac{1}{|Z_{PO+}(\mu,\nu)|} \cdot \cos\left[(\mu \cdot \rho + \nu)\omega_1 - \varphi_{PO+}(\mu,\nu)\right]\right\} \quad (18)$$

For equation 18 the following absolute values of the resistances Z_{P1} and $Z_{PO\pm}(\mu, \upsilon)$ as well as the phase shift angles φ_{P1} and $\varphi_{PO\pm}(\mu, \upsilon)$ are valid:

$$|Z_{PF}| = \sqrt{R_{LP}^2 + \left(2 \cdot \pi \cdot L_P - \frac{1}{2 \cdot \pi \cdot C_P}\right)^2} \qquad |Z_{PO\pm}(\mu,\nu)| = \sqrt{R_{LP}^2 + \left[(\mu \cdot \rho \pm \nu) \cdot 2 \cdot \pi \cdot L_P - \frac{1}{(\mu \cdot \rho \pm \nu) \cdot 2 \cdot \pi \cdot C_P}\right]^2}$$

$$\varphi_{PF} = \arctan\left(\frac{2 \cdot \pi \cdot L_P - \frac{1}{2 \cdot \pi \cdot C_P}}{R_{LP}}\right) \qquad \varphi_{PO\pm}(\mu,\nu) = \arctan\left[\frac{(\mu \cdot \rho \pm \nu) \cdot 2 \cdot \pi \cdot L_P - \frac{1}{(\mu \cdot \rho \pm \nu) \cdot 2 \cdot \pi \cdot C_P}}{R_{LP}}\right]$$

The dc-link current can be calculated with the output current of the inverter bridge and with the pulse waveforms of the phase legs - the time when the high side switches are switched-on. The pulse waveforms can be calculated if the voltage at each bridge leg is divided by the voltage U_d. Thereby it must be considered, that the output current of the other bridge leg has to be provided negative.

$$i_d(\omega_1 t) = i_P(\omega_1 t) \cdot \frac{u_{PA}(\omega_1 t) - u_{PB}(\omega_1 t)}{U_d} \quad (19)$$

In the same way the output voltage and - current and the dc-link current waveforms for control of the inverter bridge with three voltage levels can be calculate. Figure 7 show the voltage u_P and the current i_P at the output of the inverter bridge for control with two (left) and with three voltage levels (right). The phase shift angle is $\varphi_{P1} = 45°$. Beyond the waveforms the fundamental portions of the curve are included.

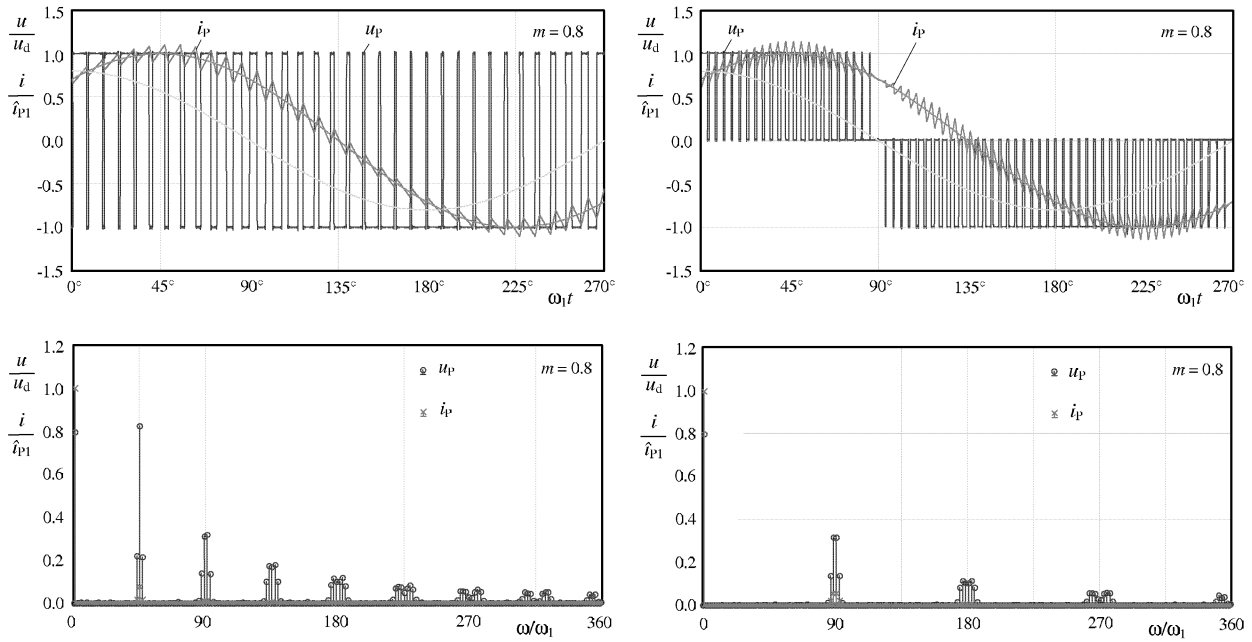

Fig. 6: Output voltage u_P and current i_P of the inverter for control with two (left) and three (right) voltage levels ($\varphi_{P1} = 45°$)

For both control strategies it can clearly be recognized that the pulsed voltage causes in approach a triangle harmonic current in the filter circuit which overlays the fundamental current. Although the

bridge legs of the inverter are controlled in both cases with the same pulse frequency ($\omega_P = 45\ \omega_1$), the output voltages spectra's below in the figure are very different. For control with two voltage levels the harmonics consist out of multiples of the pulse frequency with their sidebands. The pulse frequency at the output waveforms is doubled for control with three voltage levels, so that only multiple spectra's of the double pulse frequency and their sidebands occurs. Each of these voltage spectra entails a current whose amplitude is more and more absorbed by the filter circle with increasing frequency.

In the figure 7 the dc-link current i_d of the inverter for a sinusoidal output current is presented. For control with two voltage levels (left) the dc-link current sum is clearly higher than for control with three voltage levels (right). The spectra shows, that the dc-component and the double fundamental

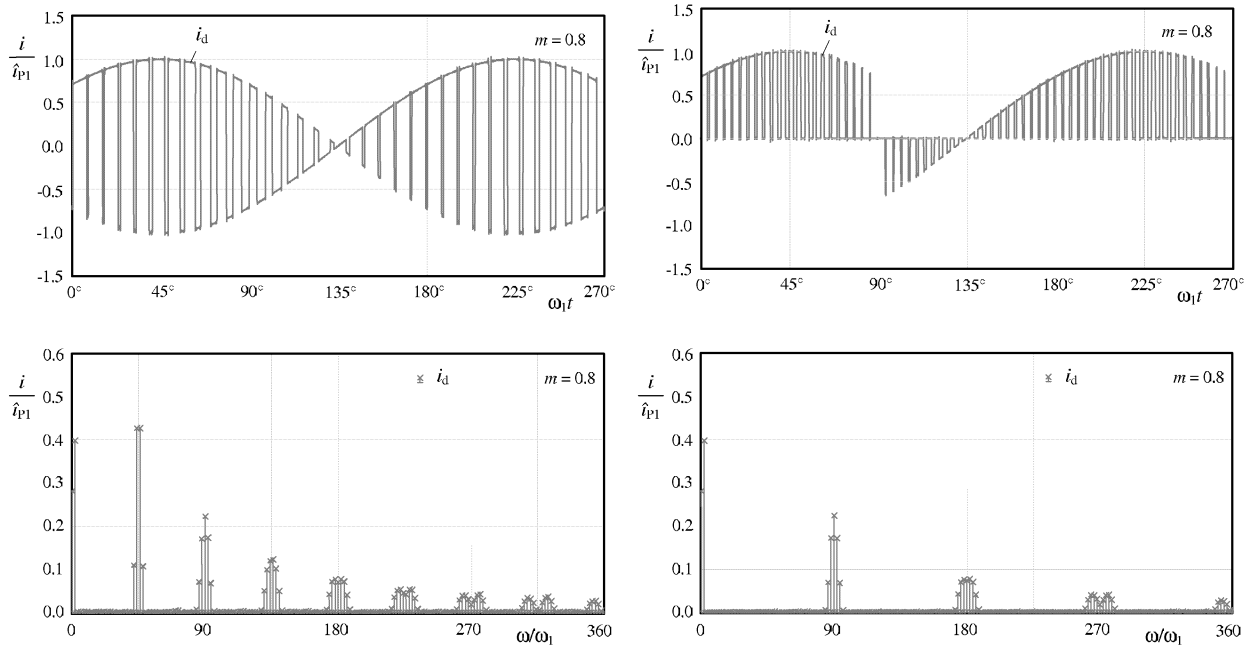

Fig. 7: Current i_d in the dc-link circuit for control with two (left) and three voltage levels (right) with sine wave output current of the inverter ($\varphi_{P1} = 45°$)

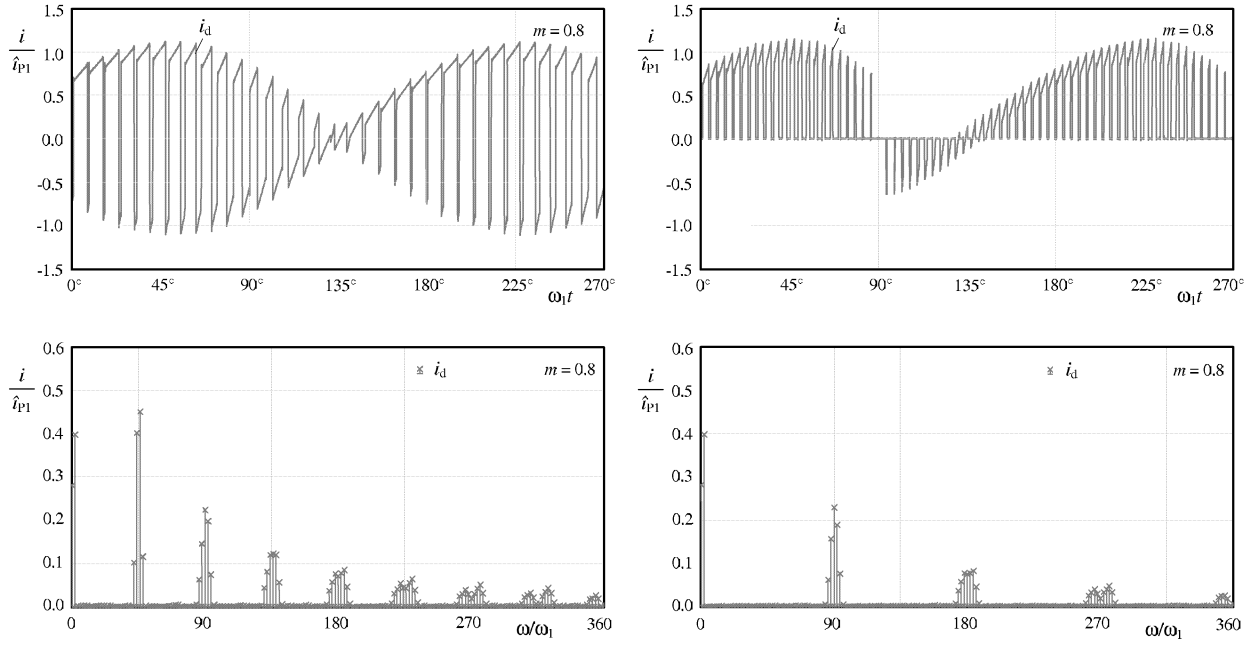

Fig. 8: Current i_d in the dc-link circuit for control with two (left) and three voltage levels (right) with overlaid harmonic output current of the inverter ($\varphi_{P1} = 45°$)

 ISBN : 90-75815-08-5

frequency portion for both control schemes is identical. However the other harmonics in the dc-link circuit differ substantially from each other. For control with two voltage levels the harmonics consist of multiples of the pulse frequency and their sidebands. In opposite to this for control with three voltage levels the pulse frequency in the dc-link circuit doubles itself. This has the consequence that multiple spectra of the double pulse frequency and their sidebands arise. With sinusoidal output current the positive and negative sidebands are arranged in each case symmetrically to each other. With consideration of the overlaid harmonic filter current at the inverter output this symmetry is lost.

Now the influence of the current harmonics at the output filter to the input current load of the inverter is calculated. Thereby it is presupposed, that the dc-current i_{d-} and the double fundamental frequency component i_{d2} flow in the input of the inverter. The individual input current harmonic components of the inverter bridge can be calculated with sinusoidal phase currents and with the sinusoidal overlaid harmonic filter currents. At first the rms-values of the amplitudes of all harmonics are to be derived and then the calculated individual portions are added geometrically.

$$I_{dO} = \sqrt{\sum_{n=3}^{\infty} \left(\frac{\hat{i}_{d\,n}}{\sqrt{2}} \right)^2} \tag{20}$$

The calculations with additional harmonic filter currents are related to them with sinusoidal current. In figure 9 the results from the calculations as a function of the load are presented with different modulation factors. The maximum current ripple specified by the design of the filter circuit amounts to 0.3 $\hat{\imath}_{AN}$. In the following figure the influence of the harmonic filter circuit current is presented for control the inverter with two (left) and three voltage levels (right).

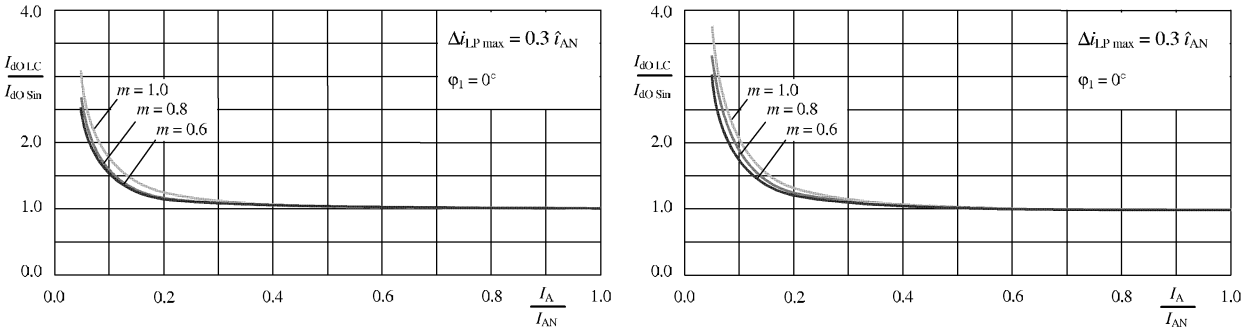

Fig. 9: Influence of the harmonic output filter current on the higher frequency dc-link current for control with two (left) und three voltage levels (right)

In the figure is clearly recognizable, that the harmonic ripple current of the filter circuit only stresses the dc-link capacitors additionally considerable with small output currents $I_A < 0.3 I_{AN}$. With larger output current the dc-link capacitor load corresponds to that with sinusoidal output current of the inverter bridge in very good approximation. For the capacitor design in the dc-link circuit for instance, these large loads are important. That means that sinusoidal output currents for the dimensions of the dc-link capacitors are sufficient. The load of the capacitors for sinusoidal output currents is presented in figure 4.

Beside the harmonic currents at the filter circuit still current harmonics arise by switching processes in the bridge legs. This current was examined in [6, 7] for single-phase inverters. At small output load of the inverter the additional current in the dc-link circuit caused by switching processes can substantially contribute to heating of the dc-link capacitors. During higher load usually again the calculated capacitor current caused by sine wave output current dominates. But no statement for all semiconductor types can be made. Beyond that this additional current contributes considerably to the pulse frequency of the inverter. The tendentious results have also their validity for a three-phase inverter [9]. For soft switching topologies an additional current in the dc-link circuit appears often. This current rises in most applications with the load of the inverter. For this reason the current must be considered mostly [10, 11].

 ISBN : 90-75815-08-5

Comparison of the Calculations with Practical Measurements

Now the calculated current in the dc-link circuit will be compared with practical measurements of an IGBT inverter. The inverter presented in figure 1, has a dc-link voltage of $U_{d-} = 108\text{V}$ and a nominal output power of $P_{AN} = 1200\text{W}$. In figure 2 the modulation scheme of the inverter for control with two (left) and with three voltage levels (right) is presented. For all switch elements in the bridge two IGBTs with internal diodes are connected in parallel. The output filter consists out of an inductor ($L_P = 125\mu\text{H}$), and some capacitors ($C_P = 14.1\mu\text{F}$). The dc-link circuit of the inverter is build out of six capacitors ($C_d = 3300\mu\text{F}$). The wiring between dc-input and power supply has a parasitic inductance.

In figure 10 the sinusoidal output values u_A and i_A as well as the input current i_E of the inverter for control with two (above) and three voltage levels (below) are presented. The inverter operates in each case with ohmic load, half nominal load (left) and nominal load (right). The dc-link voltage of 108V is approximately constant in all cases (not presented). The current in the dc-link capacitors i_{Cd} is shown below in the diagrams. The scales of the electrical values are presented right in each case, whereby the tip of each arrow marks the zero-line. The designations of the electrical values are given in figure 1.

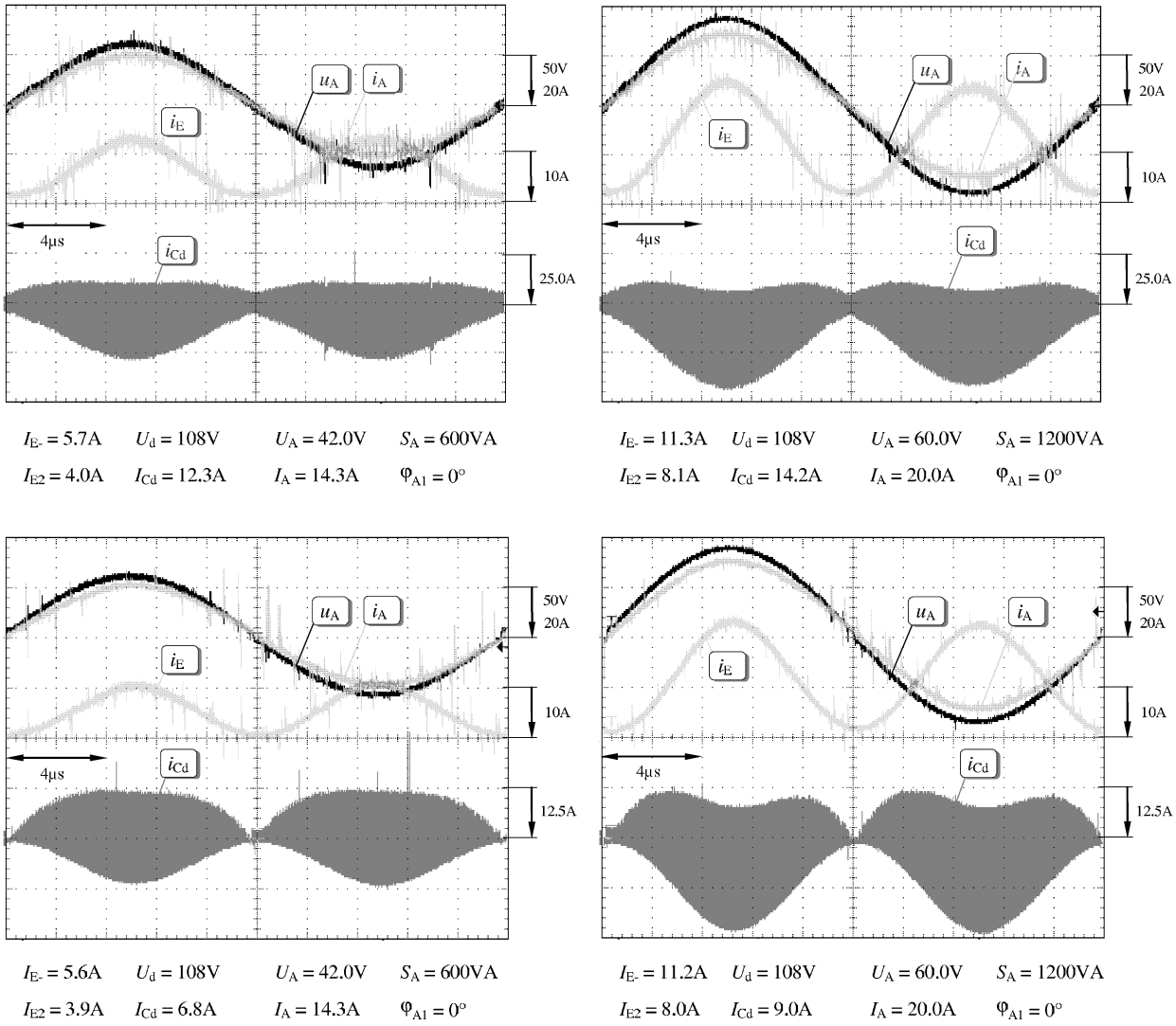

Fig. 10: Current in the dc-link capacitors as well as the input - and output values of a single-phase inverter for control with two (above) and with three voltage level (below)

The results show that the inverter input current i_E consists of a dc-component I_{E-} and a portion with double fundamental frequency i_{E2}. With increasing output power the amplitude of the double fundamental frequency becomes larger, so that the dc-portion and rms-value of the low frequency part in the H-bridge input changes. Due to the high switching frequency of the inverter the envelope curve of the capacitor current i_{Cd} is well visible. The envelope waveform repeats after a half fundamental

 ISBN : 90-75815-08-5

period. Partially a small asymmetry in the current curve can be seen. It is caused by a small portion of double fundamental current in the dc-link capacitors and by a very small phase shift angle by the output filter circuit.

All waveforms in principle correspond very well with the mathematical derivations. The results from the measurements are described below. Each plot shows also a very good correspondence to the calculated values.

Conclusion

Today pulse inverters are used world-wide in many areas for the ac-power supply. The dc-link capacitors in the power stages contribute thereby substantially to the volume, to the weight and to the costs of these inverters. For this reason the necessary size of capacitors has to be determined exactly to avoid over design. Usually the dc-link capacitor size is determined by the current load.

For single-phase bridge inverters the dc-link current in this publication has to be calculated analytically. A constant input dc-voltage as well as a sinusoidal current and voltage waveform at the output inverter is assumed. The results show, that the H-bridge input current can be split in a dc -, a double fundamental frequency - and a higher-frequency component. The dc-component flows completely in the input of the inverter. The double fundamental frequency current is split into dc-link capacitor - and inverter input component according the design of the input filter circuit. The higher-frequency current flows nearly completely through the dc-link capacitors.

The influence of inverter output harmonics, which result from the filter circuit and from the switching transitions in the inverter bridge, is examined too. It is shown, that with small output power significant capacitor load is caused by these harmonics. But with higher output power the calculated capacitor current caused by sinusoidal output current dominates again, so only a negligible additional load appears. At the end the calculations are compared with practical measurements of an IGBT inverter. A good correspondence between the calculated and measured values is shown.

References:

[1] J. Schmidt: *Einsatzbereiche, Anforderungen und Konzepte netzunabhängiger Stromversorgungen.* Seminar Haus der Technik e.V. Essen 1999

[2] F. Renken: *Einphasige Wechselrichter mit hart und weich schaltenden Transistoren für statische unterbrechungsfreie Stromversorgungen.* Dissertation Univ. der Bw. Hamburg, VDI Verlag Düsseldorf 1999, Fortschritt-Berichte ISBN 3183271214, S. 35-82

[3] M. Depenbrock: *Einphasenstromrichter mit sinusförmigem Netzstrom und gut geglätteten Gleichgrößen.* ETZ-A 1973, Band 94 S. 466-472

[4] D. Daum: *Untersuchung eines einphasigen Stromrichters mit nahezu sinusförmigen Netzstrom und gut geglätteten Gleichgrößen.* Dissertation Ruhr-Univ. Bochum 1974, S. 13-20

[5] K. Heumann: *Grundlagen der Leistungselektronik.* Lehrbuch Teubner Verlag Stuttgart 1975, 1. Auflage S. 178-182

[6] Renken F.: *Analytic Calculation of the DC-Link Capacitor Current for Pulsed Single Phase H-Bridge Inverters.* 10th EPE Meeting Toulouse, France 2-4 September 2003, Proceedings: Papers on CD ISBN 90-75815-07-7

[7] Renken F.: *Analytic Calculation of the DC-Link Capacitor Current for Pulsed Single Phase H-Bridge Inverters.* EPE Journal Volume 13 – No 4 - September - October - November 2003

[8] V. Karrer, F. Renken: *Power Electronics for the Integrated Starter Generator.* Conference: Optimization of the power train in vehicles by using the Integrated Starter Generator (ISG) Haus der Technik e. V. Munich 2002, Proceedings Expert-Verlag ISBN 3-8169-2977-2, pp. 222-247

[9] Renken F.: *Analytic Calculation of the DC-Link Capacitor Current for Pulsed Three-Phase Inverters.* 11th EPE-PEMC Meeting Riga, Latvia 2-4 September 2004

[10] M. Patt, F. Renken, J. Schmidt: *Comparison between hard and soft switched DC/AC IGBT Inverters for usage in Uninterruptible Power Supplies.* 9th EPE-PEMC Kosice 2000, Proceedings Vol. 2 pp. 34 - 39

[11] Renken F.: *Inverter with soft-switched Transistors for Uninterruptible Power Supplies.* 10th EPE Meeting Toulouse, France 2-4 September 2003, Proceedings: Papers on CD ISBN 90-75815-07-7